Title Page

SARS-CoV-2 RBD219-N1C1: A Yeast-Expressed SARS-CoV-2 Recombinant Receptor-Binding Domain Candidate Vaccine Stimulates Virus Neutralizing Antibodies and T-cell Immunity in Mice

Jeroen Pollet[1,2], Wen-Hsiang Chen[1,2], Leroy Versteeg[1], Brian Keegan[1], Bin Zhan[1,2], Junfei Wei[1], Zhuyun Liu[1], Jungsoon Lee[1], Rahki Kundu[1], Rakesh Adhikari[1], Cristina Poveda[1], Maria-Jose Villar Mondragon[1], Ana Carolina de Araujo Leao[1], Joanne Altieri Rivera[1], Portia M. Gillespie[1], Ulrich Strych[1,2], Peter J. Hotez[1,2,3,4,*], Maria Elena Bottazzi[1,2,3*]

[1] Texas Children's Hospital Center for Vaccine Development, Houston, TX, USA

[2] Departments of Pediatrics and Molecular Virology & Microbiology, National School of Tropical Medicine, Baylor College of Medicine, Houston, TX, USA

[3] Department of Biology, Baylor University, Waco, TX, USA

[4] James A. Baker III Institute for Public Policy, Rice University, Houston, TX, USA

*** Correspondence:**

Corresponding Authors

bottazzi@bcm.edu; hotez@bcm.edu

Abstract

There is an urgent need for an accessible and low-cost COVID-19 vaccine suitable for low- and middle-income countries. Here we report on the development of a SARS-CoV-2 receptor-binding domain (RBD) protein, expressed at high levels in yeast (*Pichia pastoris*), as a suitable vaccine candidate against COVID-19. After introducing two modifications into the wild-type RBD gene to reduce yeast-derived hyperglycosylation and improve stability during protein expression, we show that the recombinant protein, RBD219-N1C1, is equivalent to the wild-type RBD recombinant protein (RBD219-WT) in an *in vitro* ACE-2 binding assay. Immunogenicity studies of RBD219-N1C1 and RBD219-WT proteins formulated with Alhydrogel® were conducted in mice, and, after two doses, both the RBD219-WT and RBD219-N1C1 vaccines induced high levels of binding IgG antibodies. Using a SARS-CoV-2 pseudovirus, we further showed that sera obtained after a two-dose immunization schedule of the vaccines were sufficient to elicit strong neutralizing antibody titers in the 1:1,000 to 1:10,000 range, for both antigens tested. The vaccines induced IFN-γ, IL-6, and IL-10 secretion, among other cytokines. Overall, these data suggest that the RBD219-N1C1 recombinant protein, produced in yeast, is suitable for further evaluation as a human COVID-19 vaccine, in particular, in an Alhydrogel® containing formulation and possibly in combination with other immunostimulants.

1 Introduction

The number of coronavirus disease 19 (COVID-19) cases globally is readily approaching the 50-million-person mark, with over 1.2 million deaths. In response to the pandemic, an international enterprise to develop effective and safe vaccines is underway. There are many ways to categorize the more than 100 potential COVID-19 vaccine candidates[1], but one approach is to divide them as those employing new technologies for production, but that have not yet been licensed for use, versus traditional vaccine production approaches with prior experience in licensed vaccines[2]. The Operation Warp Speed (OWS) initiative in the United States[3] and other similar efforts in other parts of the world[4] initially seemed to focus on approaches employing new platforms, including several messenger RNA (mRNA)-based vaccines as well as non-replicating adenovirus vector vaccines[3]. Among the more established or traditional approaches, whole-inactivated virus vaccines on aluminum oxy-hydroxide have been developed in China[5], as have several recombinant protein vaccine candidates[6-8]. Each of these approaches offers both distinct advantages and disadvantages in terms of production, scale-up, potential efficacy and safety, and delivery.

We have previously reported on recombinant protein-based coronavirus vaccine candidates, formulated with Alhydrogel® to prevent severe acute respiratory syndrome (SARS)[9-11] and Middle East Respiratory Syndrome (MERS)[12]. In both cases, the receptor-binding domain (RBD) of the SARS or MERS spike proteins was used as the target vaccine antigen. In a mouse model, the SARS-CoV RBD219-N1/Alhydrogel® vaccine induced high titers of virus-neutralizing antibodies and protective immunity against a mouse-adapted SARS-CoV virus challenge. It was also found to minimize or prevent eosinophilic immune enhancement compared to the full spike protein[9].

The RBD of SARS-CoV-2 has likewise attracted interest from several groups now entering clinical trials with RBD-based vaccines[7,13-17]. Our approach was to apply the lessons learned from the development of the SARS-CoV vaccine candidate and accelerate the COVID-19 vaccine

development efforts using microbial fermentation in the yeast *Pichia pastoris*; a technology that is widely available and used to produce recombinant hepatitis B vaccines in several middle-income countries (LMICs)[18], including Bangladesh, Brazil, Cuba, India, and Indonesia. As COVID-19 spreads across the globe, especially among urban populations living in extreme poverty[19], there will be greater urgency to produce safe, effective, highly scalable, and affordable COVID-19 vaccines locally or regionally. Therefore, the development of a yeast-expressed recombinant protein-based COVID-19 vaccine allows developing it for global health and populations vulnerable to poverty-related diseases[20].

Here, we present the first preclinical data of a COVID-19 recombinant protein-based vaccine candidate, SARS-CoV2 RBD219-N1C1, formulated with Alhydrogel®. We demonstrate that modifications made to the SARS-CoV2 RBD gene to improve production and stability preserve the protein antigen functionality and its immunogenicity after Alhydrogel® adsorption.

2 Methods

2.1 Cloning and expression of the genes encoding RBD219-WT and RBD219-N1C1:

The RBD219-WT recombinant subunit protein contains amino acid residues 331-549 of the SARS-CoV-2 spike protein (GenBank No.: QHD43416.1). It contains a hexahistidine tag at its C-terminus. In the tag-free RBD219-N1C1 antigen candidate, N331 is not present, and C538 has been mutant to an alanine residue to prevent aggregation due to intermolecular disulfide bonding. The DNAs for both antigen candidates were individually synthesized with their codon use optimized for translation in *Pichia pastoris* and ligated into pPICZαA using the EcoRI and XbaI restriction sites (GenScript, Piscataway, NJ, USA). The recombinant plasmids were electroporated into *P. pastoris* X33 following the EasySelect™ Pichia Expression Kit Manual (Invitrogen, Carlsbad, CA, USA). Transformants were selected on YPD plates containing different concentrations of Zeocin (100-2000 μg/mL) and incubated at 30°C for 72 hours. Individual colonies were screened for expression under induction with methanol (0.5-2%) at the 10 mL culture level (MMGY medium) as described[10]. The expression level of select colonies was identified by SDS-PAGE and Western Blotting using anti-SARS-CoV-2 antibodies (anti-SARS-CoV-2 spike rabbit monoclonal antibody, Sino Biological, Wayne, PA, USA, Cat # 40150-R007), and research seed stocks of the highest expressing clones were frozen at –80 °C.

RBD219-WT and RBD219-N1C1 were expressed at the 5 L scale using a Celligen 310 benchtop fermentation system (Eppendorf, Enfield, CT, USA). For the RBD-WT, 2.5 L of basal salt medium were inoculated with a seed culture to an initial OD_{600} of 0.05 and grown at 30 °C, pH 5.0 with 30% dissolved oxygen until glycerol depletion. During the first hour of methanol induction, the temperature was reduced from 30 °C to 26 °C and the pH was increased from 5.0 to 6.0. After approximately 70 hours of induction (methanol feed at 1-11 mL/L/hr), the culture was harvested from the fermenter, and cells were removed by centrifugation for 30 min at 12,227 x g at 4 °C. For RBD219-N1C1, the fermentation process was slightly different in that low salt medium was used, the

induction temperature was set to 25 °C and the pH to 6.5 and, the methanol feed rate was between 1-15 ml/L/hr. The fermentation supernatant (FS) was filtered (0.45 µm PES filter) and stored at -80 °C before purification.

A hexahistidine-tagged SARS-CoV-2 RBD219-WT was purified from fermentation supernatant (FS) by immobilized metal affinity chromatography followed by size exclusion chromatography (SEC). The FS was concentrated and buffer exchanged to buffer A (20 mM Tris-HCl pH 7.5 and 0.5 M NaCl) using a Pellicon 2 cassette with a 10 kDa MWCO membrane (MilliporeSigma, Burlington, MA, USA) before being applied to a Ni-Sepharose column (Cytiva, Marlborough, MA, USA). The column was washed with buffer A plus 30 mM imidazole and elution was undertaken in buffer A containing 250 mM imidazole. The RBD219-WT protein was further purified using a Superdex 75 prep grade column (Cytiva, Marlborough, MA, USA) pre-equilibrated in buffer B (20 mM Tris-HCl pH 7.5 and 150 mM NaCl) after concentrating eluates from the Ni column using an Amicon Ultra-15 concentrator with a 10 kDa MWCO membrane (MilliporeSigma, Burlington, MA, USA). Monomeric RBD219-WT was pooled, aseptically filtered using a 0.22 µm filter, and stored at -80 °C.

For the purification of the tag-less RBD219-N1C1, ammonium sulfate salt was added to the FS to a final concentration of 1 M (w/v) before the sample was applied to a Butyl Sepharose HP column (Cytiva, Marlborough, MA, USA). The column was washed with buffer C (30 mM Tris-HCl pH 8.0) with 1 M ammonium sulfate and protein was eluted with buffer C containing 0.4 M ammonium sulfate. A polishing step using a Superdex 75 prep grade column (Cytiva, Marlborough, MA, USA) pre-equilibrated in buffer B followed.

2.2 SDS-PAGE

To evaluate the size of RBD219-WT and RBD219-N1C1, 2 μg of these two proteins were loaded onto a 4-20% tris-glycine gel under non-reduced and reduced conditions. These two proteins were also treated with PNGase-F (NEB, Ipswitch, MA, USA) under the reduced condition to remove N-glycans and loaded on the gel to assess the impact of the glycans on the protein size. Gels were stained using Coomassie Blue and analyzed using a Bio-Rad G900 densitometer with Image Lab software.

2.3 Vaccine formulation and Alhydrogel®-protein binding study

SARS-CoV-2 RBD219-N1C1 was diluted in 20 mM Tris, 150 mM NaCl, pH 7.5 (TBS buffer) before mixing with Alhydrogel® (aluminum oxy-hydroxide; Catalog # 250-843261 EP, Brenntag, Ballerup, Denmark). To calculate the Langmuir binding isotherm of RBD219-N1C1 to Alhydrogel®, RBD219-N1C1 and Alhydrogel® were mixed at different ratios (from 1:2 to 1:20). The RBD219-N1C1/Alhydrogel® mixture was stored for one hour at RT, to reach an equilibrium state. The Alhydrogel® formulations were centrifuged at 13,000 x g for 5 min, and the supernatant was removed. The protein in the supernatant fraction and the pellet fraction were quantified using a micro BCA assay (ThermoFisher, Waltham, MA, USA).

2.4 ACE-2 binding assay

For the ACE-2 binding study, the Alhydrogel®-RBD vaccine formulations were blocked overnight with 0.1% BSA. After hACE-2-Fc (LakePharma, San Carlos, CA, USA) was added, the samples were incubated for 2 hours at RT. After incubation, the Alhydrogel® was spun down at 13,000 x g for 5 min. The hACE-2-Fc which did not bind to the RBD on the Alhydrogel® remained in the supernatant. The hACE-2-Fc content in the supernatant was quantified by ELISA using 96-Well

MaxiSorp Immuno plates (ThermoFisher, Waltham, MA, USA) coated overnight with 200 ng/well of RBD219-WT protein. After blocking with 0.1% BSA, 100 µL supernatant sample were added to each well. Plates were washed 4 times with an automated plate washer using PBS with Tween (PBST). A secondary antibody against human Fc was used to detect hACE-2-Fc bound the proteins on the plate. Plates were washed 5 times with an automated plate washer using PBST before 100 µL TMB solution were added. The enzymatic reaction was stopped with HCl and absorption readings were made at 450 nm. The final concentration of the hACE-2 bound on the Alhydrogel® was determined as [hACE-2-Fc on Alhydrogel®] = [Total hACE-2-Fc] – [hACE-2-Fc in supernatant].

2.5 Immunogenicity testing

To examine RBD-specific antibodies in mouse sera, indirect ELISAs were conducted. 96-well NUNC ELISA plates were coated with 2 µg/mL RBD219-WT in 100 µL 1x coating buffer per well and incubated overnight at 4 °C. The next day the coating buffer was discarded, and plates were blocked with 200 µL/well 0.1% BSA in PBST for 2 hours at room temperature. Mouse serum samples were diluted from 1:200 to 1: 437,400 in 0.1% BSA in PBST. Blocked ELISA plates were washed once with 300 µL PBST using a Biotek 405TS plate washer and diluted mouse serum samples were added to the plate in duplicate, 100 µL/well. As negative controls, pooled naïve mouse serum (1:200 diluted) and blanks (0.1% BSA PBST) were added as well. Plates were incubated for 2 hours at room temperature, before being were washed four times with PBST. Subsequently, 1:6,000 diluted goat anti-mouse IgG HRP antibody (100 µL/well) was added in 0.1% BSA in PBST. Plates were incubated 1 hour at room temperature, before washing five times with PBST, followed by the addition of 100 µL/well TMB substrate. Plates were incubated for 15 min at room temperature while protected from light. After incubation, the reaction was stopped by adding 100 µL/well 1 M HCl. The

absorbance at a wavelength of 450 nm was measured using a BioTek Epoch 2 spectrophotometer. Duplicate values of raw data from the OD_{450} were averaged. The titer cutoff value was calculated using the following formula: Titer cutoff = 3 x average of negative control + 3 x standard deviation of the negative control. For each sample, the titer was determined as the lowest dilution of each mouse sample with an average OD_{450} value above the titer cutoff. When a serum sample did not show any signal at all and a titer could not be calculated, an arbitrary baseline titer value of 67 was assigned to that sample (baseline).

2.6 Pseudovirus assay:

Pseudovirus was prepared in HEK-293T cells by previously reported methods[21]. Cells were transfected with 2.5 µg of the plasmid encoding the SARS-CoV-2 spike protein (p278-1) and 3.7 µg of luciferase-encoding reporter plasmid (pNL4-3.lucR-E) and Gag/Pol-encoding packaging construct (pΔ8.9). Pseudovirus containing supernatant was recovered after 48 h and passed through a 0.45 µM filter before use.

For each serum sample, 30 µL pseudovirus were incubated with serial dilutions of heat-inactivated serum (eight dilutions in a 4-fold step-wise manner) for 1 h at 37 °C. Next, 100 µL of these sera-pseudovirus mixtures were added to 293T-hACE2 cells in 96-well poly-D-lysine coated culture plates. Following 48 h incubation in a 5% CO2 environment at 37 °C, the cells were lysed with 100 µL Promega Glo Lysis buffer, 15 min RT. Finally, 20 µL lysate was added to 100 µL luc substrate (Promega Luciferase Assay System, Madison, WI, USA). The amount of luciferase was quantified by luminescence (relative luminescence units (RLU)), using a Promega GloMax luminometer (Steady-Glo program). The percent virus inhibition was calculated as (1- RLU of sample/ RLU of negative control) x 100. Serum from vaccinated mice was also characterized by the IC50-value, defined as the serum dilution at which the virus infection was reduced to 50% compared

with the negative control (virus + cells). When a serum sample did not neutralize 50% of the virus when added at a 1:10 dilution, the IC50 titer could not be calculated and an arbitrary baseline titer value of 10 was assigned to that sample (baseline). As a control, human convalescent sera for SARS-CoV-2 (NIBSC 20/130) was used (National Institute for Biological Standards and Control, South Mimms, UK).

2.7 Statistical analysis

To test for significant differences between groups in ELISA, Luminex, and flow cytometry results, Kruskal-Wallis tests in combination with Dunn's multiple comparison tests were performed. ns (not significant): $p>0.05$, *: $p < 0.05$ and **: $p < 0.01$.

2.8 Cytokine analysis

2.8.1 Preparation of splenocytes for restimulation

Single-cell suspensions from mouse splenocytes were prepared using a cell dissociator (GentleMACS Octo Dissociator, Miltenyi Biotec, Waltham, MA, USA) based on a previously optimized protocol[22]. The concentration and the viability of the splenocyte suspensions were measured after mixing with AOPI dye and counted using the Nexcelom Cellometer Auto 2000 (Lawrence, MA, USA).

For the re-stimulation assays, splenocyte suspensions were diluted to $8x10^6$ live cells/mL in a 2-mL deep-well dilution plate and 125 μL of each sample was seeded in two 96-well tissue culture treated culture plates. Splenocytes were re-stimulated with 10 μg/mL RBD219-WT, 20 ng/mL PMA + 1 μg/mL Ionomycin or just media (unstimulated). For the flow cytometry plate, the PMA/I was not

added until the next day. 125 µL (2x concentration) of each stimulant was mixed with the 125 µL splenocytes suspension in the designated wells. After all the wells were prepared, the plates were incubated at 37 °C 5% CO_2. One plate was used for the cytokine release assay, while the other plate was used for flow cytometry. For flow cytometry, another plate was prepared with splenocytes, which would be later used as fluorescence minus one – controls (FMOs).

2.8.2 *In vitro* cytokine release assay

After 48 hours in the incubator, splenocytes were briefly mixed by pipetting. Then plates were centrifuged for 5 min at 400 x g at RT. Without disturbing the pellet 50 µL supernatant was transferred to two skirted PCR plates and frozen at – 20 °C until use.

For the *in vitro* cytokine release assay, splenocytes were seeded in a 96-well culture plate at $1x10^6$ live cells in 250 µL cRPMI. Splenocytes were then (re-)stimulated with either 10 µg/mL RBD219-WT protein, 10 µg/mL RBD219-N1C1 protein, PMA/Iomycin (positive control), or nothing (negative control) for 48 hours at 37 °C 5% CO_2. After incubation, 96-well plates were centrifuged to pellet the splenocytes down and supernatant was transferred to a new 96-well plate. The supernatant was stored at -20°C until assayed. A Milliplex Mouse Th17 Luminex kit (MD MilliPore) with analytes IL-1β, IL-2, IL-4, IL-6, IL-10, IL-12(p70), IL-13, IL-17A, IL-23, IFN-γ, and TNF-α was used to quantify the cytokines secreted in the supernatant by the re-stimulated splenocytes. An adjusted protocol based on the manufacturers' recommendations was used with adjustments to use less sample and kit materials[23]. The readout was performed using a MagPix Luminex instrument. Raw data was analyzed using Bio-Plex Manager software, and further analysis was done with Excel and Prism.

2.8.3 Cytokine production of activated CD4+ and CD8+ T cells

Surface staining and intracellular cytokine staining followed by flow cytometry was performed to measure the amount of activated (CD44=) CD4+ and CD8+ T cells producing IFN-γ, IL-2, TNF-α, and IL-4 upon re-stimulation with S2RBD219 WT.

Five hours before the 24-hour re-stimulation incubation, Brefeldin A was added to block cytokines from secretion. PMA/I was also added to designated wells as a positive control. After the incubation, splenocytes were stained for the relevant markers. A viability dye and an Fc Block were also used to remove dead cells in the analysis and to minimize non-specific staining, respectively.

After staining, splenocytes were analyzed using an Attune NxT flow cytometer instrument at the Baylor College of Medicine Cytometry and Cell Sorting Core. Raw data was analyzed in VenturiOne software and gating results were copied in Excel. The %-gating values from the non-stimulated controls were subtracted from the re-stimulated controls to observe the difference in %-gating induced by the re-stimulation.

The gating strategy from the analysis of the results is shown in **Supplemental Figure 1.** From all events collected the doublets are removed to obtain only single-cell events. Then events are selected on size and granularity to obtain splenocytes only. Following the removal of dead splenocytes, a gate is set to only select Activated (CD44+) T cells (CD3+)[24]. T cells are then separated into CD4+ T helper cells and CD8+ cytotoxic T cells. For T helper cells the events positive for IFN-g, TNF-a, IL-2, and IL-4 were selected, while for cytotoxic T cells only IFN-γ, TNF-α, and IL-2 positive events were gated.

3 Results

Here we report on the expression of a modified, recombinant RBD of the SARS-CoV-2 spike protein using the yeast (*P. pastoris)* expression system. The candidate antigen selection, modifications, and production processes were based on eight years of process development, manufacture, and preclinical prior experience with a SARS-CoV recombinant protein-based receptor-binding domain (RBD)[9-11]. The RBDs of the SARS-CoV-2 and SARS-CoV share significant amino acid sequence similarity (>75% identity, >80% homology) and both use the human angiotensin-converting enzyme 2 (ACE2) receptor for cell entry[25,26]. Process development using the same procedures and strategies used for the production, scale-up, and manufacture of the SARS-CoV recombinant protein allowed for a rapid acceleration in the development of a scalable and reproducible production process for the SARS-CoV-2 RBD219-N1C1 protein, suitable for its technological transfer to a manufacturer.

We found that the modifications used to minimize yeast-derived hyperglycosylation and optimize the yield, purity, and stability of the SARS-CoV RBD219-N1 protein were also relevant to the SARS-CoV-2 RBD expression and production process. The modified SARS-CoV-2 antigen, RBD219-N1C1, when formulated on Alhydrogel®, was shown to induce virus-neutralizing antibodies in mice, equivalent to those levels elicited by the wild-type (RBD219-WT) recombinant protein counterpart.

3.1 <u>Cloning and expression of the modified SARS-CoV-2 RBD</u>

The wild-type SARS-CoV-2 RBD amino acid sequence comprises residues 331-549 of the spike (S) protein (GenBank: QHD43416.1) of the Wuhan-Hu-1 isolate (GenBank: MN908947.3) (**Figure 1**). In the RBD-219-WT construct, the gene fragment was expressed in *P. pastoris*. After fermentation at the 5 L scale, the hexahistidine-tagged protein was purified by immobilized metal affinity chromatography, followed by size-exclusion chromatography. We observed glycosylation and aggregation during these initial expression and purification studies, and therefore, similar to our

previous strategy [10], we generated a modified construct, the RBD219-N1C1, by deleting the N331 residue and mutating the C538 residue to alanine. The additional mutation of C538 to A538 was done because we observed that in the wild-type sequence nine cysteine residues likely would form four disulfide bonds. Therefore, the C538 residue was likely available for intermolecular cross-linking, leading to aggregation. As a result, in the RBD219-N1C1 construct, and based on the modifications, the *Pichia*-derived hyperglycosylation, as well as aggregation via intermolecular disulfide bridging, were greatly reduced. We note that the deleted and mutated residues are structurally far from the immunogenic epitopes and specifically the receptor-binding motif (RBM) of the RBD (**Figure 1**). On SDS-PAGE tris-glycine gels, the RBD219-WT protein migrated at approximately 28 kDa under non-reduced conditions and 33 kDa in the reduced condition, while the RBD219-N1C1 protein migrated at approximately 24 kDa under non-reduced conditions and 29 kDa under reduced conditions. However, after the N-glycans were removed enzymatically, these two proteins showed a similar molecular weight of approximately 25 kDa (**Supplemental Figure 2**). The purity of both proteins was analyzed by densitometry resulting in levels >95%.

A)

```
S2-RBD       331 NITNLCPFGE VFNATRFASV YAWNRKRISN CVADYSVLYN SASFSTFKCY 380
S2-RBD-N1C1  331 -ITNLCPFGE VFNATRFASV YAWNRKRISN CVADYSVLYN SASFSTFKCY 380

S2-RBD       381 GVSPTKLNDL CFTNVYADSF VIRGDEVRQI APGQTGKIAD YNYKLPDDFT 430
S2-RBD-N1C1  381 GVSPTKLNDL CFTNVYADSF VIRGDEVRQI APGQTGKIAD YNYKLPDDFT 430

S2-RBD       431 GCVIAWNSNN LDSKVGGNYN YLYRLFRKSN LKPFERDIST EIYQAGSTPC 480
S2-RBD-N1C1  431 GCVIAWNSNN LDSKVGGNYN YLYRLFRKSN LKPFERDIST EIYQAGSTPC 480

S2-RBD       481 NGVEGFNCYF PLQSYGFQPT NGVGYQPYRV VVLSFELLHA PATVCGPKKS 530
S2-RBD-N1C1  481 NGVEGFNCYF PLQSYGFQPT NGVGYQPYRV VVLSFELLHA PATVCGPKKS 530

S2-RBD       531 TNLVKNKCVN FNFNGLTGT 549
S2-RBD-N1C1  531 TNLVKNKAVN FNFNGLTGT 549
```

B)

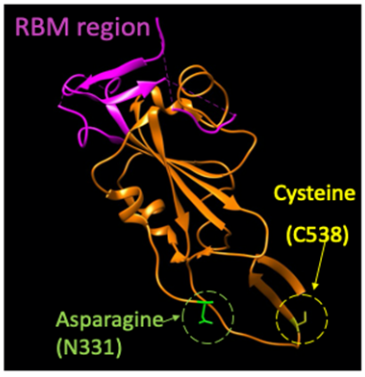

Figure 1 A) Amino acid sequence alignment between SARS-CoV-2 RBD219-WT (S2-RBD) and RBD219-N1C1 (S2-RBD-N1C1). In the N1C1-mutant, the N-terminal glutamine residue (N331, green) is removed and a C538A mutation (yellow) was introduced. Neither mutation is inside the receptor-binding motif (RBM, purple). B) The structure model of RBD219-WT was extracted from the crystal structure of the SARS-CoV-2 spike protein (PDB ID 6VXX). The RBM (N436-Y508) is again shown in

purple while the deleted asparagine (N331) and mutated cysteine (C538, mutated to alanine) in RBD219-N1C1 are highlighted in green and yellow, respectively

3.2 ACE-2 binds to recombinant SARS-CoV-2 RBD219-N1C1 protein formulated on Alhydrogel®

When mixing 25 µg of either RBD219-WT or RBD219-N1C1 proteins to 500 µg of Alhydrogel®, we observed that >98% of the proteins bind to Alhydrogel® after 15 min of incubation. Only when the Alhydrogel® was reduced to less than 100 µg (Alhydrogel®/RBD219 ratio <4), the Alhydrogel® surface was saturated, and protein started to be detected in the supernatant (**Figure 2A)**. It is known that unbound protein may impact the immunogenicity of the vaccine formulation, therefore we proceeded to only evaluate formulations with Alhydrogel®/RBD219 ratios higher than 4.

Figure 2B shows that hACE-2-Fc, a recombinant version of the human receptor used by the virus to enter the host cells, can bind with the RBD proteins that are adsorbed on the surface of the Alhydrogel®. This demonstrates that bound RBD proteins are structurally and possibly functionally active and that after adsorption the protein does not undergo any significant conformational changes that could result in the loss of possible key epitopes around the receptor-binding motif (RBM).

We saw no statistical differences between the binding of hACE-2-Fc to RBD219-WT (red, Figure 2B) or RBD219-N1C1 (green, Figure 2B) proteins, based on an unpaired t-test (P=0.670). Likewise, we saw no relation between the amount of Alhydrogel® to which the RBD was bound and the interaction with hACE-2-Fc, indicating that the surface density of the RBD proteins on the Alhydrogel® plays no role in the presentation of ACE binding sites.

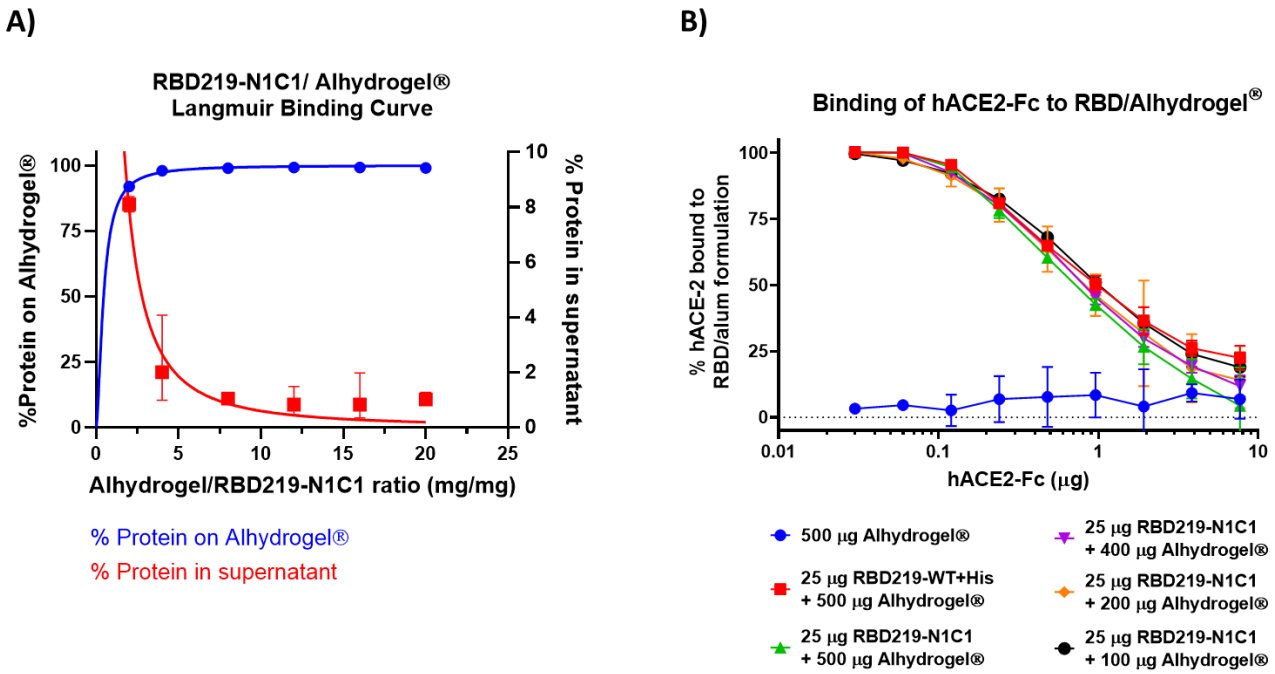

Figure 2 A) Langmuir binding isotherm of RBD219-N1C1 to Alhydrogel®. B) ELISA data, comparing the binding interaction of hACE-2-Fc to RBD219-WT bound Alhydrogel® (red) and RBD219-N1C1 bound on different amounts of Alhydrogel® (green, purple, orange, and black). Five hundred µg Alhydrogel® alone served as a negative control (blue). Data are shown as the geometric mean (n=3) with 95% confidence intervals.

3.3 Recombinant RBD219-N1C1 protein, formulated with Alhydrogel®, elicits a strong neutralizing antibody response in mice

The recombinant RBD219-N1C1 protein (25 µg) was formulated with various amounts (100 – 500 µg) of Alhydrogel®. Controls included a cohort receiving only Alhydrogel® and another receiving the RBD219-WT antigen, also formulated with 500 µg Alhydrogel®. Six- to eight-week-old female BALB/c mice were immunized 2-3 times subcutaneously at approximately 21-day intervals (**Figure 3A**). Blood samples were taken on day 35 from all study animals to assess total IgG antibody titers, as well as neutralizing antibody titers (Dataset 1). Half of the mice, those with the highest IgG titers in their respective group, were euthanized on day 43 to allow the evaluation of the cellular immune response after two immunizations. For this dataset (Dataset 2), we also measured IgG and

neutralizing antibody titers. The remaining mice received a third vaccination on day 43 and were euthanized on day 57 for the assessment of humoral and cellular immune responses (Dataset 3).

Humoral immune response: On day 35 (Dataset 1), after receiving two vaccinations, all groups that had received the recombinant protein formulated with at least 200 μg Alhydrogel® produced similar and robust IgG titers. The group receiving the protein with only 100 μg Alhydrogel®, produced a lower IgG response, albeit slightly higher than the negative control that had been immunized with 500 μg Alhydrogel® alone (**Figure 3B, Supplemental Table 1**). Importantly, based on a Mann-Whitney test, we determined that there was no statistical difference between the groups vaccinated with the modified and the wild-type version of the RBD protein (p=0.3497). The average neutralizing antibody titers observed on day 35 (IC50 range: $5.0x10^3$ to $9.4x10^3$**,** **Supplemental Table 2**) matched with the total IgG titers, showing equally high IC50 values for all vaccines that contained at least 200 μg Alhydrogel® and lower IC50 values for the vaccine with only 100 μg Alhydrogel® and no IC50 values for the adjuvant-only control (**Figure 3C**).

On day 43, 22 days after receiving the boost vaccination, half of the mice in each group (N=4), those with the highest IgG titers, were sacrificed to determine the total IgG, the IgG subtypes, and the neutralizing antibody titers. As we observed on day 35, all animals that had received the vaccine produced strong antibody titers, with the groups receiving ≥200 μg Alhydrogel® eliciting a higher titer than those that received only 100 μg of Alhydrogel®, albeit no statistical significance was detected (**Figures 3B**). For all animals, as typical for vaccine formulations containing aluminum, the IgG2a:IgG1 titer ratio was <0.1 (**Supplemental Figure 3).** In the pseudovirus neutralization assay for the day 43 samples (**Figure 3C**), all vaccines containing ≥200 μg Alhydrogel® elicited IC50 titers that, on average, were several-fold higher than on day 35 (IC50 range: $1.1x10^4$ to $1.2x10^5$, **Supplemental Table 2**). There again was no difference between the RBD219-WT and RBD-N1C1 vaccines.

On day 57, all remaining animals were sacrificed. In contrast to the animals studied on days 35 and 43, these animals had received a second boost vaccination. A robust immune response in all vaccinated mice, including those immunized with the protein adsorbed to 100 μg Alhydrogel® achieved high average IgG titers. The total IgG titers in the mice sacrificed on day 57, had increased after the third vaccination, compared to the titers seen on day 35. Likewise, we observed a corresponding increase in the average IC50 values (IC50 range: $3.8x10^2$ to $1.1x10^4$, **Supplemental Table 2**) for all animals, including those immunized with the protein adsorbed to 100 μg Alhydrogel®. Interestingly, for this time point, the cohort receiving 25 μg RBD219-N1C1 with 500 μg Alhydrogel® appeared to show higher neutralizing antibody titers than the corresponding RBD219-WT group, albeit that difference was not statistically significant.

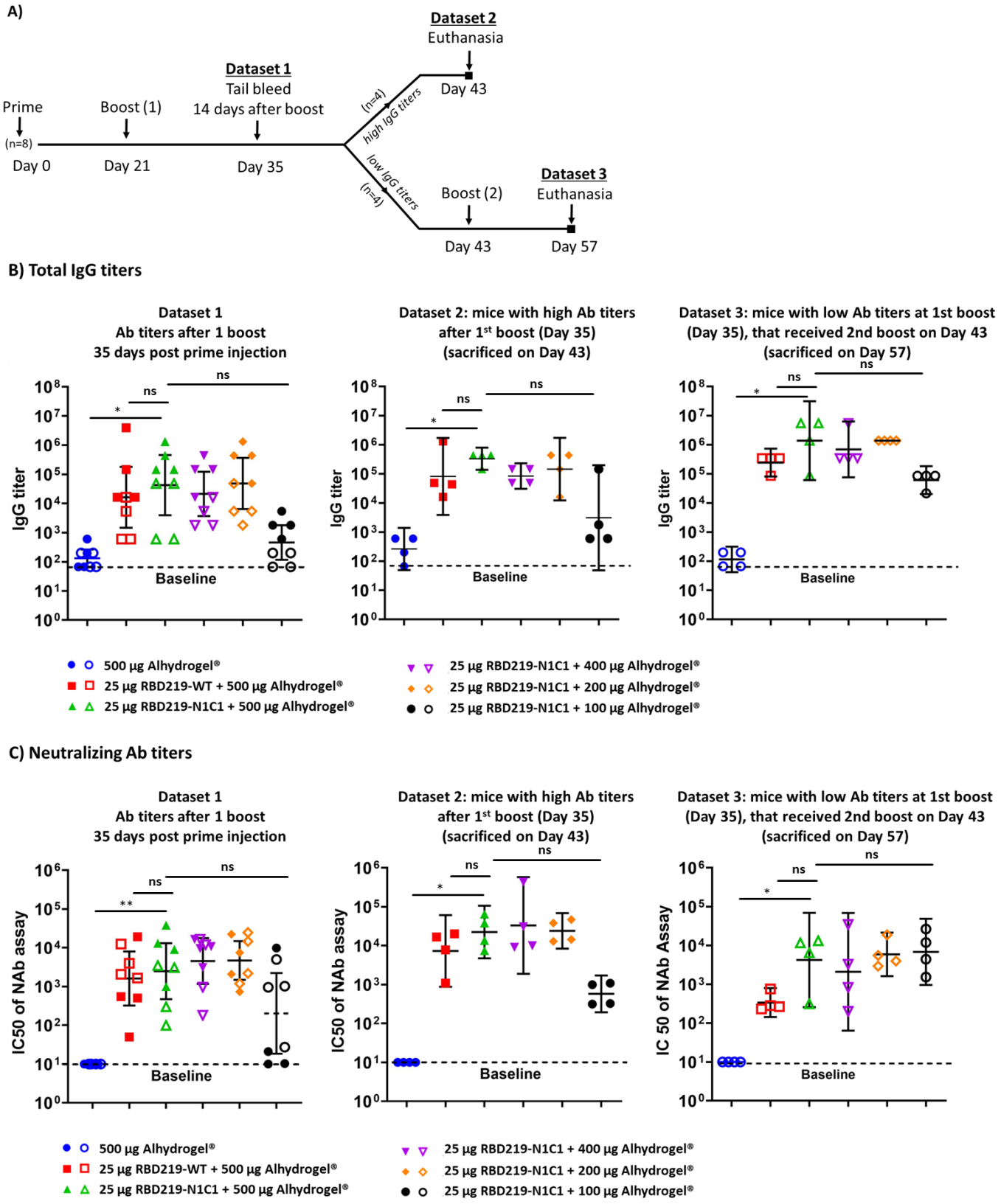

Figure 3. A) Study design. B) Total IgG titers of Datasets 1, 2, and 3 measured respectively at days 35, 43, and 57 post the prime injection. IgG titers were determined against RBD219-WT protein. Closed

data points represent data from mice with the highest IgG titers (Dataset 2), open data points represent data from mice with the lowest IgG titers (Dataset 3). C) IC50 values measured by a pseudovirus neutralization assay. Datasets 1, 2, and 3 are measured respectively at day 35, 43, and 57 after the first injection. Baselines indicate the lowest dilution measured. Lines on each group represent the geometric mean and 95% confidence intervals.

Cellular immunity: For all animals sacrificed on day 43 (having received two vaccinations) and day 57 (having received three vaccinations), the cellular immune response was characterized through the restimulation of isolated mouse splenocytes with the recombinant RBD219-WT protein. For all samples, we employed Flow Cytometry to quantify intracellular cytokines in CD4+ and $CD8^+$ cells after restimulation (**Figure 4A**). On day 43, high percentages of $CD4^+$-IL-4 and, to a slightly lesser extent $CD4^+$-TNFα producing cells were detected. Conversely, as expected for an Alhydrogel®-adjuvanted vaccine, low levels of IL-2 producing $CD4^+$ cells were seen. In a cytokine release assay, strong IFN-γ, IL-6, and IL-10 secretion was observed independent of whether the animals had received two or three immunizations, whereas low amounts of secreted Th1-typical cytokines such as IL-2 or IL-12 were seen (**Figure 4B**).

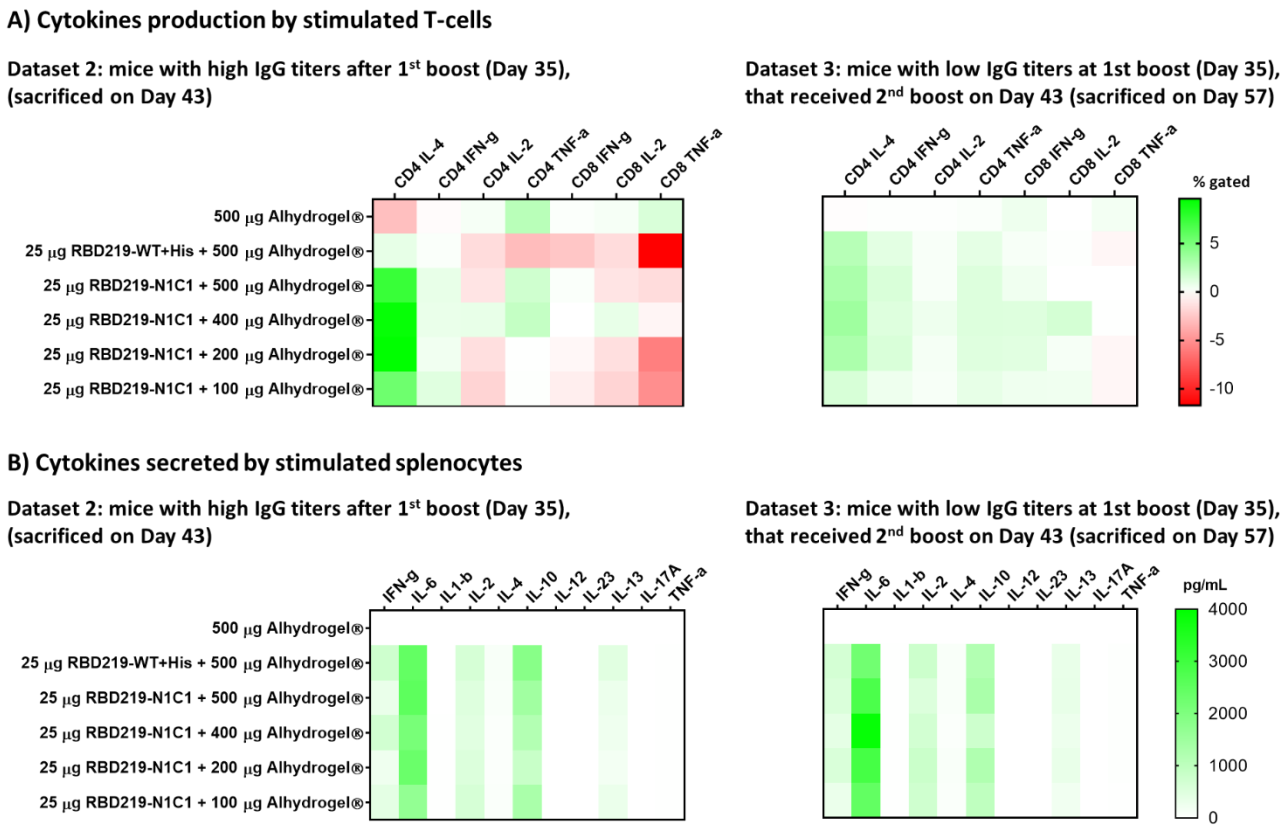

Figure 4: A) Heatmap of the cytokine response of CD4+ and CD8+ T cells after restimulation with SARS-CoV-2 RBD219-WT or RBD219-N1C1, re-stimulated splenocytes were surface and intracellularly stained and subsequently analyzed by flow cytometry. Splenocytes were obtained from mice who received two vaccinations (day 43) or three vaccinations (Day 57). Non-stimulated controls were subtracted from re-stimulated samples. B) Heatmap of secreted cytokines in supernatant from re-stimulated splenocytes from mice who received two vaccinations (day 43) or three vaccinations (Day 57). Cytokine concentrations of non-stimulated controls were subtracted from re-stimulated samples.

4 Discussion

Here we report on a yeast-expressed SARS-CoV-2 RBD219-N1C1 protein and its potential as a vaccine candidate antigen for preventing COVID-19. Building on extensive prior experience developing vaccines against SARS-CoV and MERS-CoV[10-12], we initially selected and compared the SARS-CoV-2 RBD219-WT and the SARS-CoV-2 RBD219-N1C1 proteins for their potential to induce high titers of virus-neutralizing antibodies, T-cell responses, and protective immunity.

Previously we observed that the SARS-CoV RBD219-N1 antigen, formulation with Alhydrogel® elicited high levels of neutralizing antibodies without evidence of eosinophilic immune enhancement. That RBD-based vaccine was even superior to the full-length spike protein in inducing specific antibodies and fully protected mice from SARS-CoV infection while preventing eosinophilic pulmonary infiltrates in the lungs upon challenge[9].

In this work, using the SARS-CoV-2 RBD219 protein analog, we observed that, just like in the case of the SARS-CoV RBD antigen, the deletion of the N-terminal asparagine residue reduced hyperglycosylation, thus allowing for easier purification of the antigen obtained from the yeast expression system. Moreover, mutagenesis of a free cysteine residue further improved protein production through the reduction of aggregation. Based on the predicted structure of the RBD, no impact on the functionality of the RBD219-N1C1 antigen was expected, and using an ACE-2 *in vitro* binding assay we indeed showed similarity to the RBD219-WT antigen. In addition, we showed that, in mice, the modified RBD219-N1C1 antigen triggered an equivalent immune response to the RBD219-WT protein when both proteins were adjuvanted with Alhydrogel®.

Similar to our previous findings with the SARS-CoV RBD antigen[9], we show the RBD219-N1C1 protein when formulated with Alhydrogel® elicits a robust neutralizing antibody response with IC50 values up to 4.3×10^5 in mice, as well as an expected T-cell immunological profile. Some of the

titers of virus-neutralizing antibodies exceed the titer, $2.4x10^4$, measured in-house with human convalescent serum research reagent for SARS-CoV-2 (NIBSC 20/130, National Institute for Biological Standards and Control, UK).

In a mouse virus challenge model for the SARS CoV RBD recombinant protein vaccine, we found that Alhydrogel® formulations induced high levels of protective immunity but did not stimulate eosinophilic immune enhancement, suggesting that Alhydrogel® may even reduce immune enhancement. This prior experience offers the potential for Alhydrogel® as a key adjuvant for consideration during coronavirus vaccine development[27]. Such findings have led to a reframing of the basis for immune enhancement linked to coronavirus respiratory infections[28]. A recent analysis and review by the NIH ACTIV Vaccine Working Group confirms that aluminum or Th2 responses remain viable options for vaccine development concluding that "it is not possible to clearly prioritize or down-select vaccine antigens, adjuvants, biotechnology platforms, or delivery mechanisms based on general immunological principles or the available preclinical data"[29].

Therefore, the RBD219-N1C1 vaccine antigen on Alhydrogel® merits its evaluation as a COVID-19 vaccine possibly with or without other immunostimulants. Looking at the landscape of recombinant protein-based COVID-19 vaccines, the WHO lists several advanced COVID-19 candidates that are based on recombinant proteins[30], and at least seven COVID-19 vaccines include aluminum as part of the adjuvant component[7,13,15,16,31-37], often in combination with other immunostimulants, such as CpG, to achieve a balanced immune response. Furthermore, these recombinant protein vaccines, including RBD219-N1C1, might find an additional important use as a booster if one of the newer platform vaccines, e.g., mRNA or adenovirus-based vaccines induce lower than expected immunogenicity or protection. Such prime-boost approaches have been used successfully with the chimp adenovirus vaccine for malaria and other systems, for example[38,39].

The selection of the *P. pastoris* expression platform for the production of the RBD antigen was motivated by the intent to develop a low-cost production process that could easily be transferred to manufacturers in LMICs. Currently, there are several types of COVID-19 vaccine candidates in advanced clinical trials[6,40-45]. The focus of some of the initiatives behind these vaccines is to provide vaccines for the developed world that might struggle to be successful without advanced infrastructure. Being able to match the existing experience in LMICs with the production of other biologics in yeast increases the probability of successful technology transfer[20]. For example, currently, the recombinant hepatitis B vaccine is produced in yeast by several members of the Development Country Vaccine Manufacturers Network (DCVMN), and we foresee that, given the existing infrastructure and expertise, those facilities could be repurposed to produce a yeast-produced COVID-19 vaccine[46]. Recently, the research cell bank and production process for the RBD219-N1C1 antigen was technologically transferred to a vaccine manufacturer in India and produced under cGMP conditions with the intent to enter into clinical development. In addition, preclinical studies using the RBD219-WT and RBD219-N1C1 antigens are ongoing to further optimize and evaluate other novel formulations, including a challenge study in a non-human primate model.

Acknowledgments

This work was supported by Robert J. Kleberg Jr. and Helen C. Kleberg Foundation, Fifth Generation, Inc. (Tito's Handmade Vodka), JPB Foundation, NIH-NIAID (AI14087201) and Texas Children's Hospital Center for Vaccine Development Intramural Funds.

This project was further supported by the Cytometry and Cell Sorting Core at Baylor College of Medicine with funding from the CPRIT Core Facility Support Award (CPRIT-RP180672), the NIH (CA125123 and RR024574), and the assistance of Joel M. Sederstrom. We are grateful to Drs. Munster (NIAID) and Kimata (BCM) for providing the SARS-CoV-2 pseudovirus plasmids and for technical assistance in establishing the system in our laboratory.

Author Contributions

BZ and JW planned and executed all cloning and small-scale expression studies. ZL conducted the fermentations. JL executed the protein purifications. WHC and RTK conducted the characterization of the purified proteins. JP and BK conducted mouse studies. LV, RA, MJVM, ACAL, JAR ran ELISAs. LV and CP executed the cellular assays. JP, CP, MJVM, and JAR conducted pseudovirus studies. RA and JP executed the ACE-2 binding study. MEB, JP, PJH, US, and WHC drafted the manuscript. All authors were involved in the experimental design and planning and reviewed and edited the final submission.

Data availability

All data generated or analysed during this study are included in this published article (and its supplementary information files).

Competing Interests Statement

The authors declare that Baylor College of Medicine recently licensed the RBD219-N1C1 technology to an Indian manufacturer for further development. The research conducted in this paper was performed in the absence of any commercial or financial relationships that could be construed as a potential conflict of interest.

References

1 Heaton, P. M. The Covid-19 Vaccine-Development Multiverse. *The New England journal of medicine*, doi:10.1056/NEJMe2025111 (2020).

2 Chen, W. H., Strych, U., Hotez, P. J. & Bottazzi, M. E. The SARS-CoV-2 Vaccine Pipeline: an Overview. *Current tropical medicine reports*, 1-4, doi:10.1007/s40475-020-00201-6 (2020).

3 Slaoui, M. & Hepburn, M. Developing Safe and Effective Covid Vaccines - Operation Warp Speed's Strategy and Approach. *The New England journal of medicine*, doi:10.1056/NEJMp2027405 (2020).

4 WHO. *ACCESS TO COVID-19 TOOLS (ACT) ACCELERATOR* <https://www.who.int/publications/m/item/access-to-covid-19-tools-(act)-accelerator> (2020).

5 Gao, Q. *et al.* Development of an inactivated vaccine candidate for SARS-CoV-2. *Science* **369**, 77-81, doi:10.1126/science.abc1932 (2020).

6 Keech, C. *et al.* Phase 1-2 Trial of a SARS-CoV-2 Recombinant Spike Protein Nanoparticle Vaccine. *The New England journal of medicine*, doi:10.1056/NEJMoa2026920 (2020).

7 Yang, J. *et al.* A vaccine targeting the RBD of the S protein of SARS-CoV-2 induces protective immunity. *Nature*, doi:10.1038/s41586-020-2599-8 (2020).

8 Li, T. *et al.* SARS-CoV-2 spike produced in insect cells elicits high neutralization titres in non-human primates. *Emerging microbes & infections* **9**, 2076-2090, doi:10.1080/22221751.2020.1821583 (2020).

9 Chen, W. H. *et al.* Yeast-Expressed SARS-CoV Recombinant Receptor-Binding Domain (RBD219-N1) Formulated with Alum Induces Protective Immunity and Reduces Immune Enhancement. *Vaccine* **22**, 31232-31239, doi:doi: 10.1016/j.vaccine.2020.09.061 (2020).

10 Chen, W. H. *et al.* Yeast-expressed recombinant protein of the receptor-binding domain in SARS-CoV spike protein with deglycosylated forms as a SARS vaccine candidate. *Human vaccines & immunotherapeutics* **10**, 648-658, doi:10.4161/hv.27464 (2014).

11 Chen, W. H. *et al.* Optimization of the Production Process and Characterization of the Yeast-Expressed SARS-CoV Recombinant Receptor-Binding Domain (RBD219-N1), a SARS Vaccine Candidate. *Journal of pharmaceutical sciences*, doi:10.1016/j.xphs.2017.04.037 (2017).

12 Nyon, M. P. *et al.* Engineering a stable CHO cell line for the expression of a MERS-coronavirus vaccine antigen. *Vaccine* **36**, 1853-1862, doi:10.1016/j.vaccine.2018.02.065 (2018).

13 CHICTR. *Randomized double blind, placebo controlled phase I trial for anti novel coronavirus pneumonia (COVID-19) recombinant vaccine (Sf9)*, <http://www.chictr.org.cn/showprojen.aspx?proj=60581> (2020).

14 Clinicaltrials_gov. *KBP-201 COVID-19 Vaccine Trial in Healthy Volunteers*, <https://clinicaltrials.gov/ct2/show/NCT04473690?term=Kentucky+Bioprocessing&cond=Covid19&draw=2&rank=1> (2020).

15 Clinicaltrials_gov. *A Study to Evaluate the Safety and Immunogenicity of COVID-19 (AdimrSC-2f) Vaccine*, <https://clinicaltrials.gov/ct2/show/NCT04522089> (2020).

16 Clinicaltrials_gov. *Clinical Study of Recombinant Novel Coronavirus Vaccine*, <https://clinicaltrials.gov/ct2/show/NCT04466085> (2020).

17 RPCEC. *Soberano 01 - Estudio Fase I/II, aleatorizado, controlado, adaptativo, a doble ciego y multicéntrico para evaluar la seguridad, reactogenicidad e inmunogenicidad del Candidato Vacunal profiláctico FINLAY- FR-1 anti SARS – CoV – 2 en un esquema de dos dosis. (COVID-19)*, <https://rpcec.sld.cu/ensayos/RPCEC00000332-Sp> (2020).

18 Hotez, P. J. & Bottazzi, M. E. Developing a low-cost and accessible COVID-19 vaccine for global health. *PLoS neglected tropical diseases* **14**, e0008548, doi:10.1371/journal.pntd.0008548 (2020).

19 Hotez, P. J., Bottazzi, M. E., Singh, S. K., Brindley, P. J. & Kamhawi, S. Will COVID-19 become the next neglected tropical disease? *PLoS neglected tropical diseases* **14**, e0008271, doi:10.1371/journal.pntd.0008271 (2020).

20 Hotez, P. J. & Bottazzi, M. E. *Developing a Low-Cost and Accessible COVID-19 Vaccine for Global Health*, <https://www.preprints.org/manuscript/202003.0464/v1> (2020).

21 Millet, J. K. & Whittaker, G. R. Murine Leukemia Virus (MLV)-based Coronavirus Spike-pseudotyped Particle Production and Infection. *Bio-protocol* **6**, doi:10.21769/BioProtoc.2035 (2016).

22 Jones, K. *et al.* Vaccine-Linked Chemotherapy Improves Benznidazole Efficacy for Acute Chagas Disease. *Infection and immunity* **86**, doi:10.1128/IAI.00876-17 (2018).

23 Versteeg, L. *et al.* Transferring Luminex(R) cytokine assays to a wall-less plate technology: Validation and comparison study with plasma and cell culture supernatants. *J Immunol Methods* **440**, 74-82, doi:10.1016/j.jim.2016.11.003 (2017).

24 Schumann, J., Stanko, K., Schliesser, U., Appelt, C. & Sawitzki, B. Differences in CD44 Surface Expression Levels and Function Discriminates IL-17 and IFN-gamma Producing Helper T Cells. *PLoS One* **10**, e0132479, doi:10.1371/journal.pone.0132479 (2015).

25 Zhou, P. *et al.* A pneumonia outbreak associated with a new coronavirus of probable bat origin. *Nature* **579**, 270-273, doi:10.1038/s41586-020-2012-7 (2020).

26 Hoffmann, M. *et al.* SARS-CoV-2 Cell Entry Depends on ACE2 and TMPRSS2 and Is Blocked by a Clinically Proven Protease Inhibitor. *Cell* **181**, 271-280 e278, doi:10.1016/j.cell.2020.02.052 (2020).

27 Hotez, P. J., Corry, D. B., Strych, U. & Bottazzi, M. E. COVID-19 vaccines: neutralizing antibodies and the alum advantage. *Nature reviews. Immunology* **20**, 399-400, doi:10.1038/s41577-020-0358-6 (2020).

28 Hotez, P. J., Bottazzi, M. E. & Corry, D. B. The potential role of Th17 immune responses in coronavirus immunopathology and vaccine-induced immune enhancement. *Microbes and infection*, doi:10.1016/j.micinf.2020.04.005 (2020).

29 Haynes, B. F. *et al.* Prospects for a safe COVID-19 vaccine. *Sci Transl Med*, doi:10.1126/scitranslmed.abe0948 (2020).

30 WHO. *DRAFT landscape of COVID-19 candidate vaccines*, <https://www.who.int/publications/m/item/draft-landscape-of-covid-19-candidate-vaccines> (2020).

31 Liang, J. G. *et al.* S-Trimer, a COVID-19 subunit vaccine candidate, induces protective immunity in nonhuman primates. *bioRxiv*, doi:doi: https://doi.org/10.1101/2020.09.24.311027 (2020).

32 Clinicaltrials_gov. *SCB-2019 as COVID-19 Vaccine*, <https://clinicaltrials.gov/ct2/show/NCT04405908> (2020).

33 Kuo, T. Y. *et al.* Development of CpG-adjuvanted stable prefusion SARS-CoV-2 spike antigen as a subunit vaccine against COVID-19. *bioRxiv*, doi:https://doi.org/10.1101/2020.08.11.245704 (2020).

34 Genetic_Engineering&Biotechnology_News. *COVAXX – UB-612*, <https://www.genengnews.com/covid-19-candidates/covaxx-ub-612/> (2020).

35 Clinicaltrials_gov. *A Study to Evaluate the Safety and Immunogenicity of MVC-COV1901 Against COVID-19*, <https://clinicaltrials.gov/ct2/show/study/NCT04487210> (2020).

36 Clinicaltrials_gov. *Study of the Safety, Reactogenicity and Immunogenicity of "EpiVacCorona" Vaccine for the Prevention of COVID-19 (EpiVacCorona)*, <https://clinicaltrials.gov/ct2/show/NCT04527575> (2020).

37 Clinicaltrials_gov. *A Study to Evaluate the Safety, Tolerability, and Immunogenicity of UB-612 COVID-19 Vaccine*, <https://clinicaltrials.gov/ct2/show/NCT04545749> (2020).

38 Draper, S. J. *et al.* Enhancing blood-stage malaria subunit vaccine immunogenicity in rhesus macaques by combining adenovirus, poxvirus, and protein-in-adjuvant vaccines. *Journal of immunology* **185**, 7583-7595, doi:10.4049/jimmunol.1001760 (2010).

39 Hodgson, S. H. *et al.* Combining viral vectored and protein-in-adjuvant vaccines against the blood-stage malaria antigen AMA1: report on a phase 1a clinical trial. *Molecular therapy : the journal of the American Society of Gene Therapy* **22**, 2142-2154, doi:10.1038/mt.2014.157 (2014).

40 Corbett, K. S. *et al.* SARS-CoV-2 mRNA Vaccine Development Enabled by Prototype Pathogen Preparedness. *bioRxiv*, doi:10.1101/2020.06.11.145920 (2020).

41 van Doremalen, N. *et al.* ChAdOx1 nCoV-19 vaccine prevents SARS-CoV-2 pneumonia in rhesus macaques. *Nature*, doi:10.1038/s41586-020-2608-y (2020).

42 Sadoff, J. *et al.* Safety and Immunogenicity of the Ad26.RSV.preF Investigational Vaccine Coadministered With an Influenza Vaccine in Older Adults. *The Journal of infectious diseases*, doi:10.1093/infdis/jiaa409 (2020).

43 Folegatti, P. M. *et al.* Safety and immunogenicity of the ChAdOx1 nCoV-19 vaccine against SARS-CoV-2: a preliminary report of a phase 1/2, single-blind, randomised controlled trial. *Lancet* **396**, 467-478, doi:10.1016/S0140-6736(20)31604-4 (2020).

44 Jackson, L. A. *et al.* An mRNA Vaccine against SARS-CoV-2 - Preliminary Report. *The New England journal of medicine*, doi:10.1056/NEJMoa2022483 (2020).

45 Walsh, E. E. *et al.* RNA-Based COVID-19 Vaccine BNT162b2 Selected for a Pivotal Efficacy Study. *medRxiv : the preprint server for health sciences*, doi:10.1101/2020.08.17.20176651 (2020).

46 WHO. *WHO Prequalified Vaccines*, <https://extranet.who.int/pqvdata/?AspxAutoDetectCookieSupport=1> (2020).